Noname manuscript No.
(will be inserted by the editor)

An adaptive strategy for *hp*-FEM based on testing for analyticity

T. Eibner[1], **J.M. Melenk**[2]

[1] Fakultät für Mathematik, TU Chemnitz, Reichenhainer Str. 41, D-09126 Chemnitz, Germany
[2] Department of Mathematics, PO Box 220, Reading RG6 6AX, United Kingdom

Received: date / Revised version: date

Abstract We present an *hp*-adaptive strategy that is based on estimating the decay of the expansion coefficients when a function is expanded in L^2-orthogonal polynomails on a triangle or a tetrahedron. We justify this approach by showing that the decay of the coefficients is exponential if and only if the function is analytic. Numerical examples illustrate the performance of this approach, and we compare it with two other *hp*-adaptive strategies.

Key word: adaptivity, *hp*-FEM, orthogonal polynomials on triangles and tetrahedra

1 Introduction

Over the last decades, adaptive solution strategies have become an accepted and more or less standard technique for solving partial differential equations via the finite element method. The main idea of all adaptive strategies is to start the computation with a low-dimensional approximation of the solution arising from a coarse grid on the computational domain in conjunction with low local approximation orders. Thereafter, in order to improve the accuracy of the approximation, an error indicator is employed to obtain information about the error distribution. Based on this error distribution, a suitable enlargement of the finite element space is chosen and a new approximation of higher accuracy is computed. The error of the new approximation is estimated and in case the approximation is not sufficiently accurate a new iteration of the adaptive loop is begun. In the adaptive *h*-FEM, the enlargement of the finite element space is simply done by subdividing into smaller elements all those elements that the error indicator has flagged as being tainted with a large error. However, in the *hp*-FEM one has the option to

split an element or to increase its approximation order. Thus, a main difficulty in *hp*-adaptivity is to decide whether to increase the approximation order p or to split an element whose error is large. The importance of making the correct decisions is highlighted by the *a priori* analysis of I. Babuška and B. Guo (see [6] and the monograph [30] for a survey), where it is shown that for a large class of problems an exponential rate of convergence can be achieved if the mesh and polynomial degree distribution are chosen suitably.

Generally speaking, a local p-refinement is the more efficient method on elements where the solution is smooth. On the other hand, local h-refinement is the strategy suitable for regions where the solution is not smooth. Starting from this observation, most *hp*-adaptive algorithms base the decision on whether to increase the approximation order or to refine the mesh on an estimate of the local Sobolev regularity. Estimating explicitly the local Sobolev regularity is the basis of [1–3], [8], and more recently [22, 21]. The approach of [22] generalises an idea proposed in [24], namely, to extract the regularity of the solution from the decay of the Legendre coefficients of the solution u. The work [24, 22] concentrates on one-dimensional problems and situations where all elements have tensor product structure (quadrilaterals, hexahedra); we extend this approach to triangulations consisting of triangles (in 2D) or tetrahedra (in 3D). We justify our procedure in Proposition 2 and Theorem 1 by showing that a function is analytic on the closure of a triangle/tetrahedron if and only if the coefficients of its expansion in orthogonal polynomials decay exponentially. Since the exact solution is not available, our numerical algorithm tests for exponential decay of the coefficients of the numerical solution by fitting them to an exponential decay law. The numerical studies of this paper show that an *hp*-adaptive algorithm based on testing locally for analyticity in this way works well provided the initial polynomial degree is sufficiently large.

A more implicit way of gauging the regularity of a solution underlies the algorithms of [27] and [19]. In these algorithms the solution is assumed to be smooth, and it is checked after a refinement step whether the assumption of smoothness is justified; if so, then a p-enrichment is called for in the next step, otherwise an h-refinement will be performed. The algorithm proposed in [27] is studied there for meshes consisting of quadrilaterals only and mesh refinement is facilitated by hanging nodes. The present work extends this algorithm to the case of meshes consisting of triangles.

Another adaptive strategy that we study numerically in the present paper is the application of the "three-fold" algorithm of [18].

We close this introduction by briefly mentioning related ideas for *hp*-adaptivity. The approach pursued in [11, 12] consists in formulating *hp*-adaptivity as an optimisation problem of finding the most efficient combination of h-refinement and p-enrichment. Earlier work consists of the Texas Three Step of [29, 28] and [9].

2 Model problem and *hp*-FEM

For a bounded Lipschitz domain $\Omega \subset \mathbb{R}^2$ and $f \in L^2(\Omega)$ we consider the following Dirichlet problem, given in weak formulation:

Problem 1 (model problem) Find $u \in H^1_0(\Omega)$ such that

$$\int_\Omega \nabla u \cdot \nabla v \mathrm{d}\Omega = \int_\Omega f v \mathrm{d}\Omega \qquad \forall\, v \in H^1_0(\Omega). \tag{1}$$

We will restrict our considerations to γ-shape-regular triangulations $\mathcal{T}$ of Ω consisting of affine triangles. That is, each element $K \in \mathcal{T}$ is the image $F_K(\hat{K})$ of the reference triangle $\hat{K}$, and we have

$$h_K^{-1} \|F_K'\|_{L^\infty(K)} + h_K \|(F_K')^{-1}\|_{L^\infty(K)} \leq \gamma \qquad \forall\, K \in \mathcal{T},$$

where h_K denotes the diameter of the element K. In order to define *hp*-FEM spaces on a mesh $\mathcal{T}$, we associate a polynomial degree $p_K \in \mathbb{N}$ with each element $K \in \mathcal{T}$ and collect these p_K in the polynomial degree vector $\mathbf{p} := (p_K)_{K\in\mathcal{T}}$. We furthermore associate with each edge e of the triangulation a polynomial degree

$$p_e := \min\{p_K \,|\, \text{e is an edge of element } K\} \tag{2}$$

and denote by

$$\mathbf{p}(K) := (p_{e1}, p_{e2}, p_{e3}, p_K) \tag{3}$$

the vector containing the polynomial distribution of the triangle $K \in \mathcal{T}$ with edges $\{e_i \mid i = 1,2,3\}$. Next, we introduce the reference triangle $\hat{K}$ and the reference square $\hat{Q}$ by

$$\hat{K} := \{(x,y) \mid -1 < x, y \ \wedge\ x + y < 0\}, \qquad \hat{Q} := (-1,1)^2 \tag{4}$$

and point out the following relationship between these reference elements:

Lemma 1 (Duffy transformation) *The transformation $D : \mathbb{R}^2 \to \mathbb{R}^2$ given by*

$$D : (\eta_1, \eta_2) \mapsto (\xi_1, \xi_2) = \left(\frac{1}{2}(1+\eta_1)(1-\eta_2) - 1, \eta_2\right)$$

maps $\hat{Q}$ onto $\hat{K}$. The inverse transformation $D^{-1} : \mathbb{R}^2 \to \mathbb{R}^2$ is given by

$$D^{-1} : (\xi_1, \xi_2) \mapsto (\eta_1, \eta_2) = \left(2\frac{1+\xi_1}{1-\xi_2} - 1, \xi_2\right).$$

Now we are in the position to define local shape functions on the reference triangle $\hat{K}$. To do so, we proceed as follows:

1. We define a set Φ of functions on the reference square $\hat{Q}$.
2. We transform these functions via $D : \mathbb{R}^2 \to \mathbb{R}^2$ given by Lemma 1 to functions on the reference triangle $\hat{K}$.

Fig. 1 Reference elements $\hat{K}$ and $\hat{Q}$

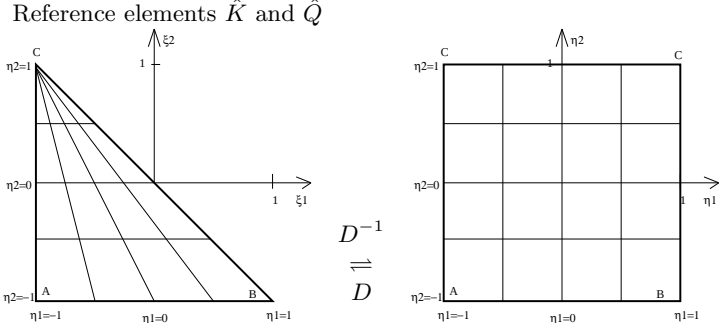

Definition 1 (Local shape functions on the reference triangle) *Let the reference elements $\hat{K}$, $\hat{Q}$ be given by (4) and let the transformation $D : \mathbb{R}^2 \to \mathbb{R}^2$ be given by Lemma 1. Then, for a degree vector $\mathbf{p}(\hat{K}) = (p_{AB}, p_{AC}, p_{BC}, p_K)$, where $p_{AB}, \ldots, p_{BC}$ denote the polynomial degrees associated with the edges $AB, \ldots, BC$ and p_K denotes the polynomial degree associated with the interior of the triangle, we define a set of local shape functions as follows:*

$$\Psi^B := \Phi^B \circ D^{-1} = \left\{ \phi \circ D^{-1} | \phi \in \Phi^B \right\} \quad B = 1, \ldots, 5,$$

with Φ^B given by:

$$\Phi^1 = \left\{ \frac{(1-\eta_1)}{2}\frac{(1-\eta_2)}{2}, \frac{(1+\eta_1)}{2}\frac{(1-\eta_2)}{2}, \frac{(1+\eta_2)}{2} \right\},$$

$$\Phi^2 = \left\{ \frac{(1-\eta_1)}{2}\frac{(1+\eta_1)}{2}\frac{(1-\eta_2)^2}{4} P_{i-1}^{(1,1)}(\eta_1) \mid i = 1, \ldots, p_{AB} - 1 \right\},$$

$$\Phi^3 = \left\{ \frac{(1-\eta_1)}{2}\frac{(1-\eta_2)}{2}\frac{(1+\eta_2)}{2} P_{j-1}^{(1,1)}(\eta_2) \mid j = 1, \ldots, p_{AC} - 1 \right\},$$

$$\Phi^4 = \left\{ \frac{(1+\eta_1)}{2}\frac{(1-\eta_2)}{2}\frac{(1+\eta_2)}{2} P_{j-1}^{(1,1)}(\eta_2) \mid j = 1, \ldots, p_{BC} - 1 \right\},$$

$$\Phi^5 = \left\{ \frac{(1-\eta_1^2)}{4}\frac{(1+\eta_2)}{2}\left(\frac{1-\eta_2}{2}\right)^{i+1} P_{i-1}^{(1,1)}(\eta_1) P_{j-1}^{(2i+1,1)}(\eta_2) \right.$$
$$\left. \mid i, j = 1, \ldots, p_K - 1 \right\};$$

here, $P_i^{(\alpha,\beta)}(\eta)$ is the i-th Jacobi polynomial with respect to the weight $(1-\eta)^\alpha(1+\eta)^\beta$.

The subdivision of the shape functions into 5 different groups in Definition 1 follows a standard pattern in *hp*-FEM:

– Φ^1 contains the vertex shape functions, which are the usual linear shape functions, equal to one in exactly one node and zero in the other nodes.

- The sets Φ^2, Φ^3, Φ^4 contain the side shape functions, which are zero in all nodes and vanish on all but one edge.
- The set Φ^5 consists of internal shape functions, which vanish on $\partial\hat{K}$.

Properties of this set of shape functions are collected in the following lemma.

Lemma 2 *For $B = 1, \ldots, 5$ let Ψ^B be given by Definition 1. Denote by*

$$\mathcal{P}_p(\hat{K}) = span\{x^i y^j \mid 0 \le i + j \le p\}, \qquad \mathcal{P}_p(I) = span\{x^i \mid 0 \le i \le p\}$$

the spaces of all polynomials of degree p and set

$$\mathcal{P}_{\mathbf{p}(\hat{\mathbf{K}})}(\hat{K}) = \{\psi \in \mathcal{P}_{p_K}(\hat{K}) \mid \psi|_{e_i} \in \mathcal{P}_{p_{e_i}}(e_i), i = 1, \ldots, 3\},$$
$$\tilde{\mathcal{Q}}_{\mathbf{p}(\hat{K})}(\hat{K}) = span\ \Psi := span\left\{\bigcup_{B=1}^{5} \Psi^B\right\},$$

where e_i, $i = 1, \ldots, 3$ denote the edges of $\hat{K}$. Then

1. *$\Psi := \bigcup_{B=1}^{5} \Psi^B$ is a set of linear independent functions,*
2. *$\mathcal{P}_{\mathbf{p}(\hat{\mathbf{K}})}(\hat{K}) \subset \tilde{\mathcal{Q}}_{\mathbf{p}(\hat{K})}(\hat{K})$,*
3. *$\psi \in \Psi$ is polynomial.*

Proof To prove the statements above we can proceed as in [23].

Remark 1 The vertex and side shape functions introduced in Definition 1 are those proposed by G. Karniadakis and S. Sherwin, [23]. The internal shape functions Φ^5 differ from those of [23] in that we admit roughly twice as many internal shape functions. Our reason for using this bigger space is that the shape functions of Φ^5 can be modified so as to be adapted to the quadrature rule employed. The stiffness matrix can then be set up in optimal complexity. These ideas have been presented for reference elements with tensor product structure (squares, hexahedra) in [26] and can be generalised to the present situation of triangles and tetrahedra, [15]. We emphasise that the additional shape functions are all internal shape functions that can be eliminated on the element level by static condensation.

Our conforming *hp*-FEM spaces are defined as follows:

Definition 2 (FEM spaces) *Let $\mathcal{T}$ be a regular mesh consisting of triangles, and let $\mathbf{p}$ be a polynomial degree vector. Furthermore, for all edges e let p_e be given by (2). Then we set*

$$S^{\mathbf{p}}(\Omega, \mathcal{T}) := \{u \in H^1(\Omega) \mid u \circ F_K \in \tilde{\mathcal{Q}}_{\mathbf{p}(K)}(\hat{K}) \quad \forall K \in \mathcal{T}\},$$
$$S_0^{\mathbf{p}}(\Omega, \mathcal{T}) := S^{\mathbf{p}}(\Omega, \mathcal{T}) \cap H_0^1(\Omega),$$

with $\tilde{\mathcal{Q}}_{\mathbf{p}(K)}(\hat{K})$ defined in Lemma 2.

Remark 2 We remark that the use of the Duffy transformation implies an unsymmetry, since one of the vertices of the triangle is special, namely, the vertex corresponding to the vertex C of the reference triangle. This in turn implies that the space $S^{\mathbf{p}}(\Omega, \mathcal{T})$ of Definition 2 is not completely described. In our implementation, the vertices of the triangulation are globally numbered (arbitrarily). The element maps are then chosen such that the vertex with the lowest global number corresponds to vertex A of the reference element and the vertex with the highest global number corresponds to the degenerate vertex C.

The FE-discretisation of Problem 1 then reads:

Problem 2 (hp-FEM approximation) Find $u_h \in S_0^{\mathbf{p}}(\Omega, \mathcal{T})$ such that

$$\int_\Omega \nabla u \cdot \nabla v \mathrm{d}\Omega = \int_\Omega f v \mathrm{d}\Omega \qquad \forall\, v \in S_0^{\mathbf{p}}(\Omega, \mathcal{T}).$$

3 Error indicator

This section is devoted to the residual-based a-posteriori error estimator used in the *hp*-adaptive algorithms of Section 4 to decide which elements to refine. The error estimator was developed in [27] and so we refer to [27] for a detailed description.

Definition 3 (error estimator) *Let $K \in \mathcal{T}$. Then the local error indicator η_K, associated with the element K is given by:*

$$\eta_K^2 := \eta_{B_K}^2 + \eta_{E_K}^2,$$

where the first term $\eta_{B_K}^2$ is the weighted internal residual and the second term $\eta_{E_K}^2$ a weighted boundary residual. They are given by

$$\eta_{B_K}^2 := \frac{h_K^2}{p_K^2} \left\| f_{p_K} + \Delta u_{FE} \right\|_{L^2(K)}^2 \quad \textit{and} \quad \eta_{E_K}^2 := \sum_{e \subset \partial K \cap \Omega} \frac{h_e}{2p_e} \left\| [\frac{\partial u_{FE}}{\partial n_e}] \right\|_{L^2(e)}^2,$$

where f_K denotes the $L^2(K)$-projection of f on the space of polynomials of degree $p_K - 1$ and $[\frac{\partial u_{FE}}{\partial n_e}]$ the jump of the normal derivative of u_{FE} across the edge e. Finally, the global error indicator is given by

$$\eta^2 := \sum_{K \in \mathcal{T}} \eta_K^2.$$

The following proposition collects the most important properties of the error indicator η:

Proposition 1 *Let $\epsilon > 0$. Let $\mathcal{T}$ be a γ-shape-regular mesh. Assume that the polynomial degree distribution satisfies*

$$\frac{1}{\gamma} p_K \leq p_{K'} \leq \gamma p_K \qquad \forall K, K' \text{ with } \overline{K} \cap \overline{K'} \neq \emptyset.$$

Then there exist $C_1, C_2 > 0$ independent of h and $\mathbf{p}$ such that

$$\|u - u_{FE}\|^2_{H^1(\Omega)} \leq C_1 \sum_{K \in \mathcal{T}} \eta_K^2 + \frac{h_K^2}{p_K^2} \|f - f_{p_K}\|^2_{L^2(K)},$$

$$\eta_K^2 \leq C_2(\epsilon) p_K^{1+2\epsilon} \left(p_K \|u - u_{FE}\|^2_{H^1(\omega_K)} + p_K^{2\epsilon} \frac{h_K^2}{p_K^2} \|f_{p_K} - f\|^2_{L^2(\omega_K)} \right).$$

3.1 Performance of the error indicator

In this subsection we present some numerical results to demonstrate the performance of the error indicator given in Definition 3. We introduce three examples:

Example 1 We consider Problem 1 on $\Omega_S = (0,1)^2$ together with a right-hand side f chosen such that the exact analytic solution is given by

$$u = x(1-x)y(1-y)(1-2y)e^{-\frac{5}{2}(2x-1)^2}.$$

Example 2 We consider Problem 1 on $\Omega_L = (0,1)^2 \backslash ([0,1] \times [-1,0])$ together with a right-hand side f chosen such that the exact solution u is

$$u = r^{\frac{2}{3}} \sin\left(\frac{2}{3}\varphi\right) \left(1 - r^2 \cos^2 \varphi\right) \left(1 - r^2 \sin^2 \varphi\right).$$

We note that $u \in \cap_{\epsilon > 0} H^{5/3-\epsilon}(\Omega_L)$.

Example 3 For $\Omega = (-1,1) \times (0,1)$, $\Gamma_N = (-1,1) \times \{0\}$, $\Gamma_D = \partial\Omega \backslash \Gamma_N$ and

$$g_N(x,y) = -\frac{2}{3} g\left(r \cos\phi\right) \cos\left(-\frac{1}{3}\phi\right) r^{-\frac{1}{3}}$$

$$g(t) = \begin{cases} -at^3 - bt^2 - ct - d : t < -0.8 \\ 1 : |t| \leq 0.8 \\ at^3 - bt^2 + ct - d : t > 0.8 \end{cases},$$

with $(a,b,c,d) = (250, 675, 600, 175)$, we consider the problem: Find $u \in V := \{u \in H^1(\Omega) \mid u|_{\Gamma_D} = 0\}$ such that

$$\int_\Omega \nabla u \cdot \nabla v \mathrm{d}\Omega = \int_\Omega f v \mathrm{d}\Omega + \int_{\Gamma_N} g_n v \mathrm{d}\Gamma \qquad \forall\, v \in H_0^1(\Omega),$$

where f is chosen such that the exact solution u is

$$u(r,\phi) = g(r\cos\phi) g(r \sin\phi) r^{\frac{2}{3}} \sin\left(\frac{2}{3}\phi\right).$$

We note that $u \in \cap_{\epsilon > 0} H^{5/3-\epsilon}(\Omega)$.

For a fixed polynomial degree p the error indicator η reduces to a standard h-FEM error indicator and therefore we are mainly interested in the p-dependence of η. In order to examine the p-dependence of η, we consider a pure p-FEM on a mesh consisting of 4 triangles in the case of Example 1, a mesh consisting of 12 triangles in the case of Example 2, and the mesh shown in Fig. 3 for Example 3. The important property of the mesh for Example 3 is that, in contrast to Example 2, the singularity is *not* at a mesh point. The results of our computation are plotted in Figures 2 and 3. All plots show the global error measured in the H^1-norm and the error predicted by η. As we can see, in each example the true error is overestimated by η and especially in Example 2 we observe that as the polynomial degree p increases, the true error decays much faster then the error indicator η predicts. Note, however, that Proposition 1 is suboptimal in the efficiency estimate so that η is allowed to overestimate the error. The situation of Example 2 is special: The solution is in some Sobolev space $H^k(\Omega)$, (here: $k = 5/3 - \epsilon$), but the singularity is located at a mesh point; it is known from approximation theory that singularity functions of the type considered here can be approximated in the H^1-norm by polynomials of degree p with an error $O(p^{-2(k-1)})$; this convergence is faster than the $O(p^{-(k-1)})$ behaviour achievable for generic functions in H^k, [7], [30, Sec. 3.3.5]. In Example 3, the singularity is not located at a mesh point. We observe in Fig. 3 and from the effectivity indices in Table 1 that in this situation the indicator η captures the true error accurately.

Fig. 2 p-performance of the error indicator (cf. Examples 1, 2)

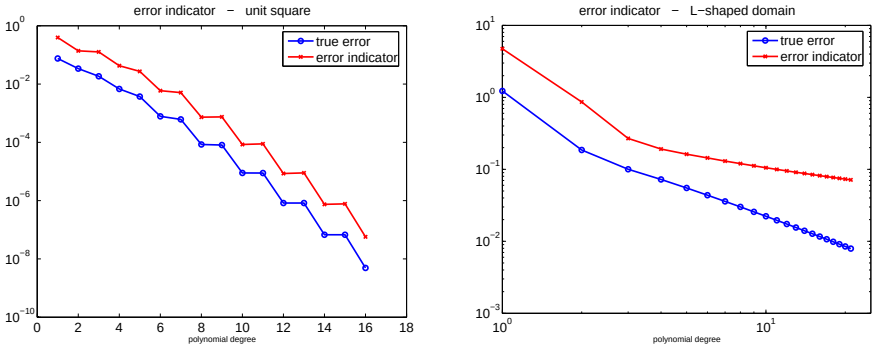

4 *hp*-adaptive strategies

In this section we investigate and compare three different hp-adaptive strategies. For each of these strategies we use the error indicator $\eta^2 := \sum_{K\in\mathcal{T}} \eta_K^2$ defined in Section 3 to determine which elements need to be refined. While

Fig. 3 Example 3: mesh and p-performance of the error indicator

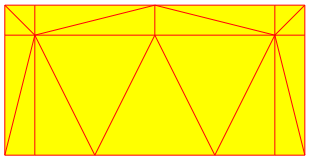

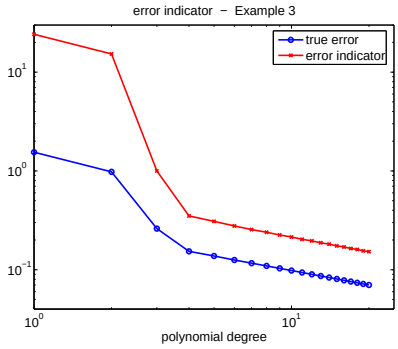

Table 1 effectivity index $\eta/\|u-u_{FE}\|_{H^1(\Omega)}$

p	Ex. 1	Ex. 2	Ex. 3	p	Ex. 1	Ex. 2	Ex. 3
1	5.22	3.85	15.70	11	10.02	5.09	3.09
2	4.08	4.64	15.73	12	10.27	5.47	3.18
3	6.83	2.67	4.64	13	10.77	5.85	3.12
4	6.24	2.64	3.33	14	11.02	6.24	3.20
5	7.31	2.94	3.16	15	11.47	6.62	3.15
6	7.62	3.29	3.21	16	11.62	7.02	3.22
7	8.26	3.63	3.06	17	11.95	7.41	3.18
8	8.66	3.99	3.17	18	—	7.81	3.25
9	9.19	4.35	3.07	19	—	8.21	3.20
10	9.49	4.72	3.16	20	—	8.61	3.27

the three adaptive strategies differ in the way they decide whether to perform an *h*- or a *p*-refinement, the basic adaptive loop in all three cases is the following:

Algorithm 1 (basic *hp*-adaptive algorithm)

– *Input: An admissible mesh* $\mathcal{T}$ *together with a polynomial degree distribution* $\mathbf{p} := (p_K)_{K\in\mathcal{T}}$ *and the corresponding finite element solution* $u_{FE} \in S_0^{\mathbf{p}}(\Omega,\mathcal{T})$.
– *Output: The refined mesh* $\mathcal{T}_{ref}$ *together with the polynomial degree distribution* $\mathbf{p} := (p_K)_{K\in\mathcal{T}_{ref}}$.
– *Algorithm:*
  1. *Calculate the error indicator* η_K^2 *for all* $K \in \mathcal{T}$.
  2. *Determine* $\mathcal{T}_{h\_ref} \subset \mathcal{T}$ *containing all* $K \in \mathcal{T}$ *selected for h-refinement.*
  3. *Determine* $\mathcal{T}_{p\_ref} \subset \mathcal{T}$ *containing all* $K \in \mathcal{T}$ *selected for p-refinement.*
  4. *Compute a preliminary version of the refined mesh* $\mathcal{T}_{ref}$ *by subdividing all* $K \in \mathcal{T}_{h\_ref}$ *into four congruent sons (red refinement).*
  5. *Determine the refined mesh* $\mathcal{T}_{ref}$ *by eliminating hanging nodes.*

6. *Increase the polynomial degree* $p_K := p_K + 1$ *for all elements* $K \in \mathcal{T}_{ref} \cap \mathcal{T}_{p\_ref}$. *(In particular: elements to which an h-refinement is applied inherit the polynomial degree from their father).*

Algorithm 2 (elimination of hanging nodes) *The elimination of hanging nodes is done as follows:*

1. *While there exists an element* $K \in \mathcal{T}_{h\_ref}$ *with more than one hanging node subdivide this element into four congruent sons (red refinement).*
2. *Subdivide all elements* $K \in \mathcal{T}_{h\_ref}$ *with one hanging node into two sons (green refinement).*

Remark 3 Since green refinement divides an interior angles of the father element into two angles of about half the size of the original angle, repeated use of green refinement may lead to a degeneration of the mesh. In order to avoid such a degeneration, we forbid further refinement of triangles resulting from a green refinement. Instead of subdividing a so-called green triangle, we undo the green refinement and perform a red subdivision of the father element before further refinement may occur. (For further information about adaptive mesh refinement strategies see [17] and the references therein.)

Remark 4 The *hp*-adaptive Algorithm 1 is restricted to shape-regular meshes and isotropic polynomial degrees. The design of *hp*-adaptive algorithms with anisotropic elements and/or anisotropic polynomial degrees, while highly desirable, is beyond the scope of the present paper. For different aspects of anisotropy in low-order FEM such as *a posteriori* error estimation and adaptivity, we mention the recent [10,16,5,4] and the references therein. Concerning anisotropic polynomial degrees, we point out that they are much more naturally employed in connection with quadrilateral and hexahedral elements. Then, the analog of our Strategy II below can be formulated where regularity in each variable is gauged separately; we refer to [22] for the details. Also the fully general *hp*-adaptive approach of [11] conceptually generalises to meshes consisting of triangles.

Having presented the basic *hp*-algorithm, we consider different strategies for determining $\mathcal{T}_{h\_ref}$, the set of all triangles selected for h-refinement, and $\mathcal{T}_{p\_ref}$, the set of all triangles selected for p-refinement.

4.1 Strategy I - Comparison of estimated and predicted error

The first strategy we consider is the strategy proposed in [27]. The decision whether to split an element or to increase its approximation order is based on comparing the current estimated error with a prediction from a previous step of the adaptive loop:

Algorithm 3 *For chosen parameters* σ, γ_h, γ_p *and* γ_n *do:*

1. Compute the mean error

$$\overline{\eta}^2 = \frac{1}{\#\mathcal{T}} \sum_{K \in \mathcal{T}} \eta_K^2.$$

2. Determine

$$\mathcal{T}_{p\_ref} = \left\{ K \in \mathcal{T} \mid \eta_K^2 \geq \sigma \overline{\eta}^2 \wedge \eta_K^2 < \left(\eta_K^{pred}\right)^2 \right\},$$
$$\mathcal{T}_{h\_ref} = \left\{ K \in \mathcal{T} \mid \eta_K^2 \geq \sigma \overline{\eta}^2 \wedge \eta_K^2 \geq \left(\eta_K^{pred}\right)^2 \right\}.$$

For the predicted error of the initial triangulation we set

$$\eta_K^{pred} = \begin{cases} 0 \text{ if we prefer } h\text{-refinement for the first refinement step} \\ \infty \text{ if we prefer } p\text{-refinement for the first refinement step} \end{cases},$$

and after each adaptive refinement step, i.e., after finishing step 6 of the basic adaptive algorithm, we update the error prediction via the following algorithm:

Algorithm 4 (error prediction) *For all $K \in \mathcal{T}$ do*

– *If K is h-refined, then for all K_s = son of K set*

$$\left(\eta_{K_s}^{pred}\right)^2 := \left(\eta_K^{pred}\right)^2 \cdot \begin{cases} \frac{1}{4}\gamma_h \left(\frac{1}{2}\right)^{2p_K} & \textit{in the case of red subdivision} \\ \frac{1}{2} & \textit{in the case of green subdivision} \end{cases}. \tag{5}$$

– *If K is p-refined, then*

$$\left(\eta_K^{pred}\right)^2 := \gamma_p \left(\eta_K^{pred}\right)^2. \tag{6}$$

– *If no refinement is done, then*

$$\left(\eta_K^{pred}\right)^2 := \gamma_n \left(\eta_K^{pred}\right)^2.$$

Remark 5 (undoing green refinements) As discussed in Remark 3, the *h*-refinement of an element that has undergone a green refinement in a previous step of the adaptive loop is done by first recombining this element K with its sibling K_{sib} to obtain the father element K_{father} and then performing a red refinement for this father element. The error prediction then proceeds analogously: the intermediate element K_{father} is assigned $(\eta_{K_{father}}^{pred})^2 := (\eta_K^{pred})^2 + (\eta_{K_{sib}}^{pred})^2$ and the four sons of K_{father} are then assigned predictions according to the red subdivision case in (5).

Our computation of η_K^{pred} follows the lines of [27] in the event of a red subdivision or a p-refinement. In the case of a green refinement we observe that the triangle K is subdivided into two triangles without significantly reducing the edge length or the diameter. Thus, we don't expect a considerable error reduction and merely assign half the error of K to each of its sons. The motivation for the decision between h- and p-refinement is the following: The predictions (5) and (6) assume maximal smoothness of the solution; in fact the prediction (6) assumes analyticity of the solution so that the error can decay exponentially. If the estimated error is smaller than the predicted error, then we perform p-refinement since the assumption of smoothness appears to be correct. Otherwise, if the estimated error is larger than the predicted error, we perform h-refinement since our assumption of smoothness does not seem to be correct.

4.2 Strategy II - Decay of Legendre expansion coefficients

The second second strategy we consider is to determine whether the solution is locally smooth (analytic) or not by expanding the finite element solution in orthogonal polynomials. This idea was first discussed in [24] (see also [22, 21]). The theoretical basis for the case of triangular elements is the following result:

Proposition 2 *Define on the reference triangle $\hat{K}$ the $L^2(\hat{K})$-orthogonal basis ψ_{pq}, p, $q \in \mathbb{N}_0$ by*

$$\psi_{pq} = \tilde{\psi}_{pq} \circ D^{-1} \quad \text{with } \tilde{\psi}_{pq} = P_p^{(0,0)}(\eta_1) \left(\frac{1-\eta_2}{2}\right)^p P_q^{(2p+1,0)}(\eta_2),$$

where $P_p^{(\alpha,\beta)}(\eta)$ denotes the p-th Jacobi polynomial with respect to the weight $(1-\eta)^\alpha(1+\eta)^\beta$ and D the transformation of Lemma 1. Let $u \in L^2(\hat{K})$ be written as $u = \sum_{p,q\in\mathbb{N}_0} u_{pq}\psi_{pq}$. Then u is analytic on $\overline{\hat{K}}$ if and only if there exist constants C, $b > 0$ such that $|u_{pq}| \le Ce^{-b(p+q)}$ for all p, $q \in \mathbb{N}_0$.

Proof Combine [25, Prop. 3.2.14] and [25, Lemma 3.2.15].

We will present the extension of Proposition 2 to tetrahedra below in Theorem 1. The main idea of an *hp*-algorithm that is based on estimating the decay of the coefficients is to check whether the expansion coefficients u_{pq} of $(u_{FE}|_K) \circ F_K = \sum_{p,q} u_{pq}\psi_{pq}$ decay sufficiently fast. If so, then an exponential convergence in p can be expected and a p-refinement is indicated. Otherwise, an h-refinement is called for. Since the exact solution $u|_K$ is not available, we will consider the expansion of the finite element approximation. This leads to:

Algorithm 5 *For parameters σ and δ do:*

1. Compute the mean error

$$\overline{\eta}^2 = \frac{1}{\#\mathcal{T}} \sum_{K \in \mathcal{T}} \eta_K^2.$$

2. For all elements $K \in \mathcal{T}$ with $\eta_K^2 \geq \sigma \overline{\eta}^2$ compute the expansion coefficients

$$u_{ij;K} = \|\psi_{ij}\|_{L^2(\hat{K})}^{-2} \big(u_{FE}|_K \circ F_K^{-1}, \psi_{ij}\big)_{L^2(\hat{K})}, \quad 0 \leq i+j \leq p_K$$

and estimate the decay coefficient b_K by a least-squares fit of

$$\ln |u_{ij;K}| \sim C_K - b_K(i+j).$$

3. Determine

$$\mathcal{T}_{p\_ref} = \{K \in \mathcal{T} \mid \eta_K^2 \geq \sigma \overline{\eta}^2 \wedge b_K \geq \delta\},$$
$$\mathcal{T}_{h\_ref} = \{K \in \mathcal{T} \mid \eta_K^2 \geq \sigma \overline{\eta}^2 \wedge b_K < \delta\}.$$

4.3 Strategy III - Three-fold algorithm

The third strategy we consider goes back to an idea proposed in [18] for the treatment of hypersingular and weakly singular integral equations arising in the context of boundary element methods. In contrast to the previous strategies, the decision which elements should be refined is no longer based on a mean value strategy. Instead, the crucial value for refinement is the maximum occurring error. The main idea of the algorithm is: If the error indicator η_K predicts a small error for $K \in \mathcal{T}$ (with respect to the maximum occurring error), we do nothing. For elements with medium predicted error we perform a *p*-enrichment and those elements with a large predicted error are *h*-refined. Thus, the algorithm reads as follows:

Algorithm 6 *For parameters δ_1, δ_2 with $0 < \delta_1 < \delta_2 < 1$ do:*

1. Compute the maximum error

$$\eta_{max}^2 = \max_{K \in \mathcal{T}} \eta_K^2.$$

2. Determine

$$\mathcal{T}_{p\_ref} = \{K \in \mathcal{T} \mid \delta_1 \eta_{max}^2 \leq \eta_K^2 \leq \delta_2 \eta_{max}^2\},$$
$$\mathcal{T}_{h\_ref} = \{K \in \mathcal{T} \mid \eta_K^2 > \delta_2 \eta_{max}^2\}.$$

4.4 Numerical results

In this section the performance of each adaptive *hp*-strategy from above is tested for two very different problems. The first example we consider is Example 1. Since we have an analytic solution, the optimal strategy is a pure p-method on a suitable mesh, which features an exponential convergence in the polynomial degree p. We therefore expect a successful *hp*-algorithm to perform only a few h-refinements at the beginning and then turn into a pure p-method in later iterations. Anticipating an exponential convergence in p we plot the error versus $\sqrt{\text{DOF}}$. The second example we consider is Example 2, the classical L-shaped domain. In this case we have a singularity at the origin and so we expect a strong mesh refinement towards this reentrant corner in conjunction with p-refinement for the rest of the domain. For this example, the best known *hp*-strategy yields an error bound of

$$\|u - u_{FE}\|_{H^1(\Omega)} \leq Ce^{-b(\text{DOF})^{1/3}}$$

(see, e.g., [30]); for this example, therefore, we plot the error versus $(\text{DOF})^{1/3}$. All computations are performed with the *hp*-FEM code ADURACON, [14]. We now consider the strategies in detail:

- **Strategy I:** For our computations we choose: $\sigma = 0.75$, $\gamma_p = 0.7$, $\gamma_h = 4.0$ and $\gamma_n = 1.0$ together with $\eta_K^{pred} = 0$ for all $K \in \mathcal{T}$. The corresponding results are shown in Tables 2, 3 and Figures 4-6, 13, 16, 19. As we observe, Strategy I performs well in both cases. In the case of Example 1 we obtain the expected p-method after a few mesh refinement steps; Example 2 features a strong mesh refinement towards the singularity at the reentrant corner and p-refinement in the remainder of the domain where the solution is smooth. In comparison to the other strategies, we obtain a slightly increased number of h-refinements and relatively large polynomial degree of $p_K \in \{4; 5\}$ for the elements at the reentrant corner. A possible reason for the increasing number of h-refinements in Table 2 at higher iteration levels could be limitations of computational accuracy. In such a case the error does not decrease further and consequently the algorithm always suggests h-refinement.
- **Strategy II:** The computations are based on: $\sigma = 0.75$, $\delta = 1.0$. Moreover, in order to obtain a sufficient number of Legendre expansion coefficients, which is necessary to achieve a good estimate for the decay coefficient b, we start with an initial polynomial degree distribution $p_K = 3$ for all $K \in \mathcal{T}$. As we can see (Table 4, Figure 7 and following), for both cases, Example 1 and Example 2, the algorithm performs well. In Example 1 the error appears to have reached the limit of computational accuracy after 18 iterations.
- **Strategy III:** For our computations we choose: $\delta_1 = 0.07$, $\delta_2 = 0.7$. We observe that in the case of Example 2 the algorithm performs well but it performs a considerable number of h-refinements for the analytic solution on the unit square. However, this "failure" is predictable: If we

consider Algorithm 6, we observe that the algorithm is not designed for problems whose solution is smooth on the whole domain. In fact, it is impossible to achieve pure p-enrichment since for nearly uniform error distributions the algorithm opts for a pure h-refinement. This happened, for example, in Level 13.

Remark 6 Throughout all computations we observed that the majority of the wrong decisions concerning h- or p- refinement, in particular an increase of the polynomial degree in regions where the solution is not smooth, occur in the initial steps of the iteration. Wrong decisions in later stages are rather an exception. (See the mesh and polynomial degree distribution near the reentrant corner of the L-shaped domain.) We therefore expect an improvement by combining the strategies above with an appropriate coarsening algorithm that corrects excessive p-refinement in regions where the solution is not smooth.

Fig. 4 Strategy I - L-shaped domain - Iteration levels 0, 15, and 25

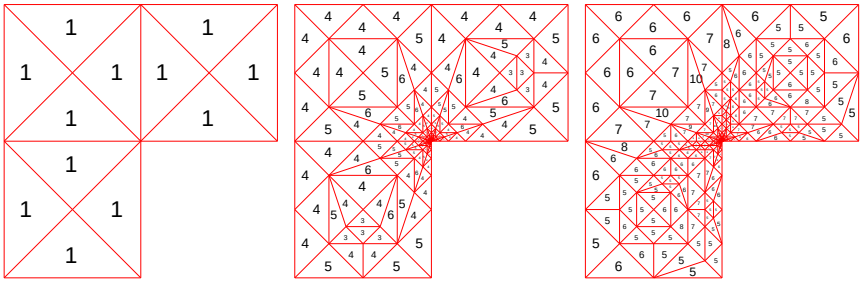

Fig. 5 Strategy I - L-shaped domain - zoom near reentrant corner: Iteration levels 15 (magnification factor 2^9) and 25 (magnification factor 2^{19})

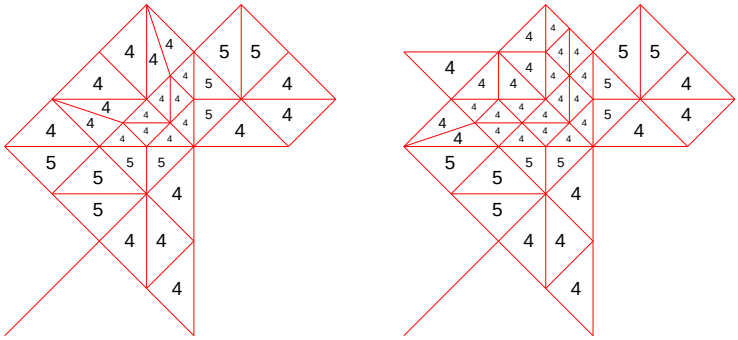

Fig. 6 Strategy I - unit square - Iteration levels 0, 10, and 20

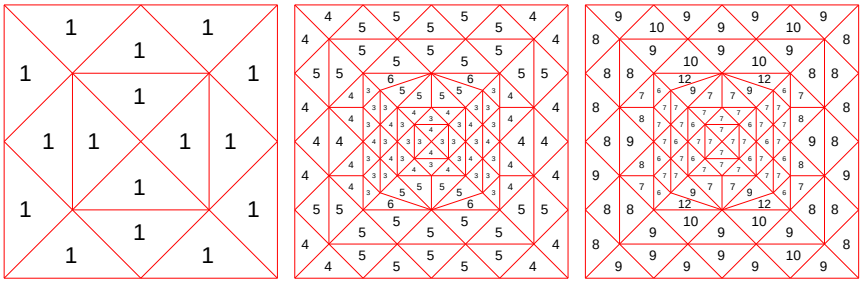

Table 2 Strategy I - L-shaped domain - Number of elements, maximum polynomial degree, h- and p-refinements per level

Level	$\#\mathcal{T}$	p_{max}	h_{ref}	p_{ref}	Level	$\#\mathcal{T}$	p_{max}	h_{ref}	p_{ref}
0	12	1	12	0	13	238	5	14	10
1	40	1	8	26	14	262	6	14	20
2	48	2	8	14	15	286	6	22	36
3	60	3	0	26	16	318	7	14	32
4	60	3	0	20	17	342	7	14	28
5	60	4	6	16	18	366	7	14	34
6	70	5	14	12	19	390	8	42	42
7	94	5	14	8	20	442	8	34	50
8	118	5	14	12	21	490	9	32	50
9	142	5	14	20	22	536	10	18	54
10	166	5	14	10	23	568	10	26	78
11	190	5	14	14	24	612	10	26	80
12	214	5	14	8	25	656	10	36	82

Table 3 Strategy I - unit square - Number of elements, maximum polynomial degree, h- and p-refinements per level

Level	$\#\mathcal{T}$	p_{max}	h_{ref}	p_{ref}	Level	$\#\mathcal{T}$	p_{max}	h_{ref}	p_{ref}
0	16	1	12	0	11	104	6	0	33
1	40	1	12	14	12	104	6	0	35
2	52	2	12	12	13	104	7	0	32
3	64	2	16	23	14	104	8	0	41
4	92	3	8	37	15	104	9	0	37
5	104	3	0	50	16	104	9	0	49
6	104	4	0	36	17	104	9	0	49
7	104	4	0	34	18	104	10	0	37
8	104	5	0	44	19	104	11	0	36
9	104	5	0	42	20	104	12	0	42
10	104	6	0	46					

Fig. 7 Strategy II - L-shaped domain - Iteration levels 0, 15, and 25

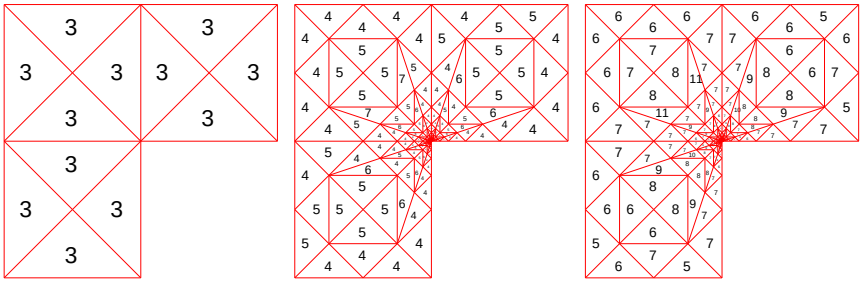

Fig. 8 Strategy II - L-shaped domain - zoom near reentrant corner: Iteration levels 15 (magnification factor 2^{11}) and 25 (magnification factor 2^{21})

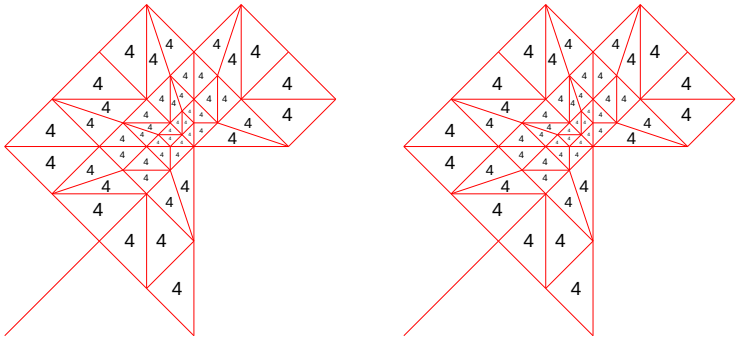

Fig. 9 Strategy II - unit square - Iteration levels 0, 10 and 20

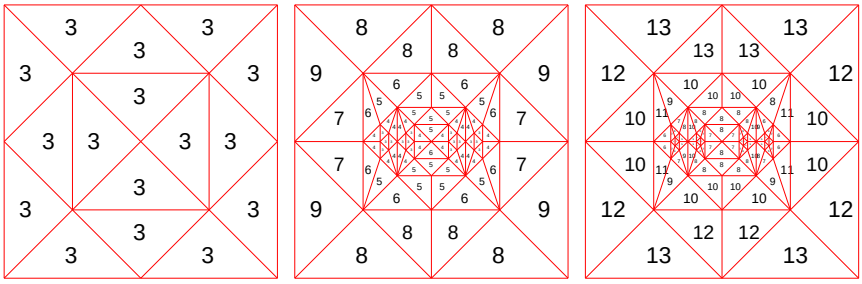

Table 4 Strategy II - L-shaped domain - Number of elements, maximum polynomial degree, h- and p-refinements per level

Level	$\#\mathcal{T}$	p_{max}	h_{ref}	p_{ref}	Level	$\#\mathcal{T}$	p_{max}	h_{ref}	p_{ref}
0	12	3	10	0	13	292	6	16	20
1	30	3	10	4	14	316	6	16	28
2	40	4	14	2	15	340	7	16	44
3	58	4	12	0	16	364	7	16	42
4	76	4	16	0	17	388	8	16	48
5	100	4	16	0	18	412	8	16	48
6	124	4	16	0	19	436	8	16	68
7	148	4	16	14	20	460	9	16	68
8	172	4	16	20	21	484	9	16	76
9	196	4	16	10	22	508	9	16	80
10	220	5	16	6	23	532	9	16	100
11	244	5	16	2	24	556	10	16	92
12	268	5	16	14	25	580	11	16	112

Table 5 Strategy II - unit square - Number of elements, maximum polynomial degree, h- and p-refinements per level

Level	$\#\mathcal{T}$	p_{max}	h_{ref}	p_{ref}	Level	$\#\mathcal{T}$	p_{max}	h_{ref}	p_{ref}
0	16	3	0	4	11	80	9	16	33
1	16	4	8	4	12	104	9	0	28
2	32	4	0	8	13	104	10	0	34
3	32	5	0	16	14	104	10	0	42
4	32	6	12	4	15	104	11	0	34
5	56	6	0	16	16	104	11	0	26
6	56	6	0	12	17	104	12	0	24
7	56	7	0	34	18	104	13	0	43
8	56	8	16	9	19	104	13	0	44
9	80	8	0	28	20	104	13	0	47
10	80	9	0	24					

Fig. 10 Strategy III - L-shaped domain - Iteration levels 0, 15, and 25

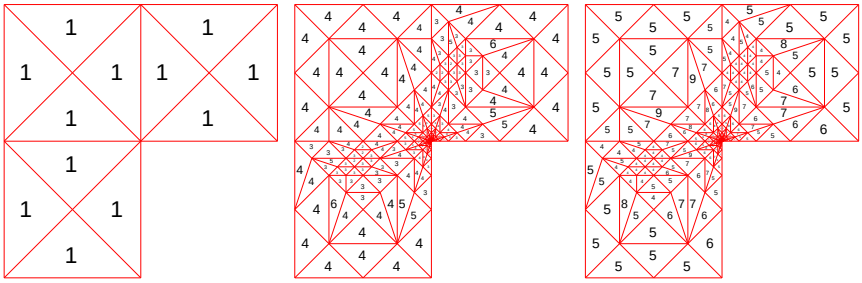

Fig. 11 Zoom near reentrant corner - Iteration level 15 (magnification factor 2^9) - Iteration level 25 (magnification factor 2^{19})

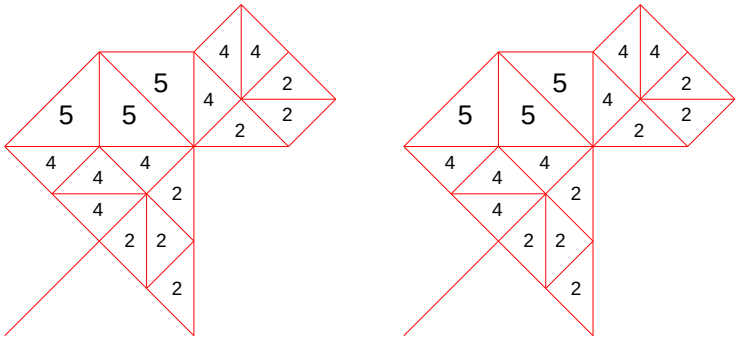

Fig. 12 Strategy III - unit square - Iteration levels 0, 10, and 20

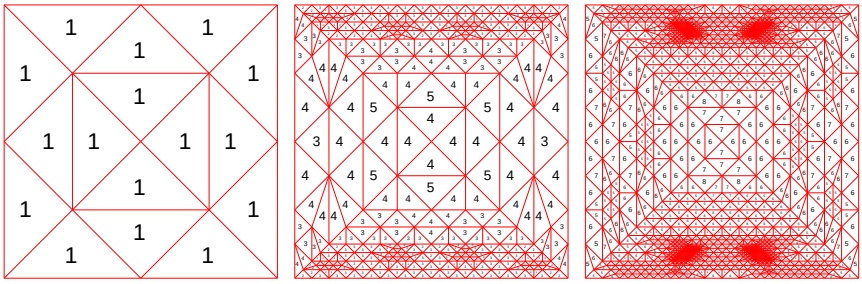

Table 6 Strategy III - L-shaped domain - Number of elements, maximum polynomial degree, h- and p-refinements per level

Level	$\#\mathcal{T}$	p_{max}	h_{ref}	p_{ref}	Level	$\#\mathcal{T}$	p_{max}	h_{ref}	p_{ref}
0	12	1	6	2	13	262	6	14	32
1	26	2	8	18	14	286	6	14	36
2	34	2	12	10	15	310	6	14	28
3	52	3	16	18	16	334	6	14	46
4	68	4	28	14	17	358	6	14	40
5	112	4	6	42	18	382	7	14	44
6	118	5	12	10	19	406	7	14	48
7	136	5	6	2	20	430	8	14	40
8	142	5	14	8	21	454	8	14	56
9	166	5	14	18	22	478	8	14	82
10	190	5	14	22	23	502	8	14	66
11	214	5	14	32	24	526	8	14	82
12	238	5	14	34	25	550	9	14	96

Table 7 Strategy III - unit square - Number of elements, maximum polynomial degree, h- and p-refinements per level

Level	$\#\mathcal{T}$	p_{max}	h_{ref}	p_{ref}	Level	$\#\mathcal{T}$	p_{max}	h_{ref}	p_{ref}
0	16	1	8	0	11	512	6	144	115
1	28	1	12	12	12	768	7	48	135
2	40	2	12	20	13	832	7	500	92
3	64	3	44	12	14	1868	7	20	8
4	132	3	68	44	15	1888	7	68	951
5	240	3	64	104	16	1972	7	16	152
6	340	4	56	104	17	2000	7	164	182
7	408	4	28	48	18	2208	7	40	40
8	444	4	16	36	19	2248	7	204	258
9	460	4	16	202	20	2564	8	16	495
10	476	5	24	132					

Fig. 13 Strategy I - Performance of *hp*-adaptive algorithm

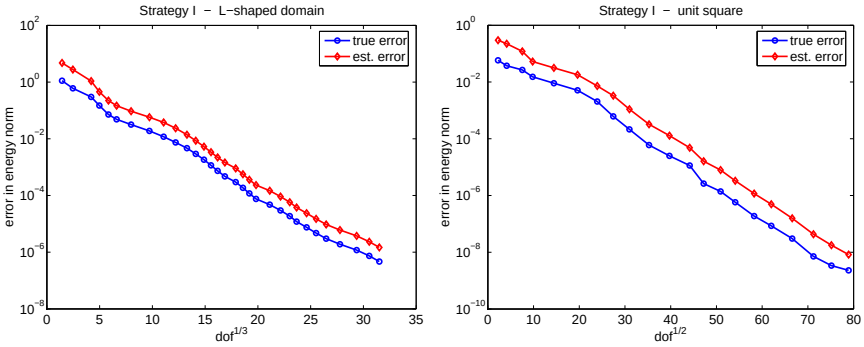

Fig. 14 Strategy II - Performance of *hp*-adaptive algorithm

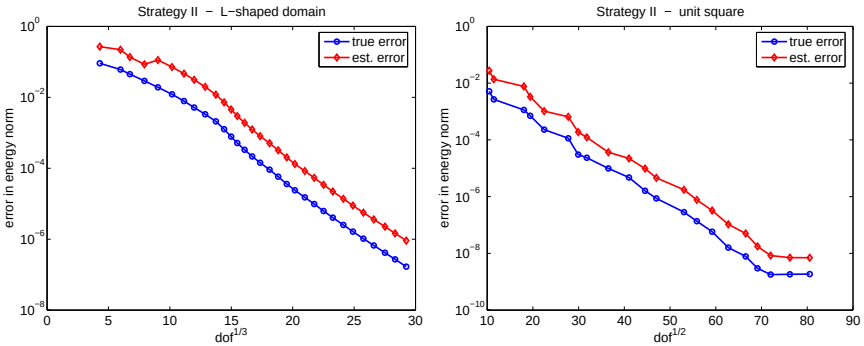

Fig. 15 Strategy III - Performance of *hp*-adaptive algorithm

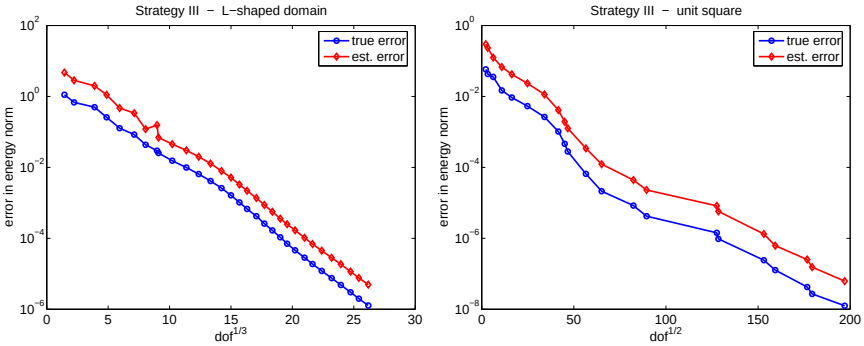

Fig. 16 Strategy I - L-shaped domain - Polynomial degree distribution along the line from (0,0) to (-1/2,1) - Iteration levels 15 and 25

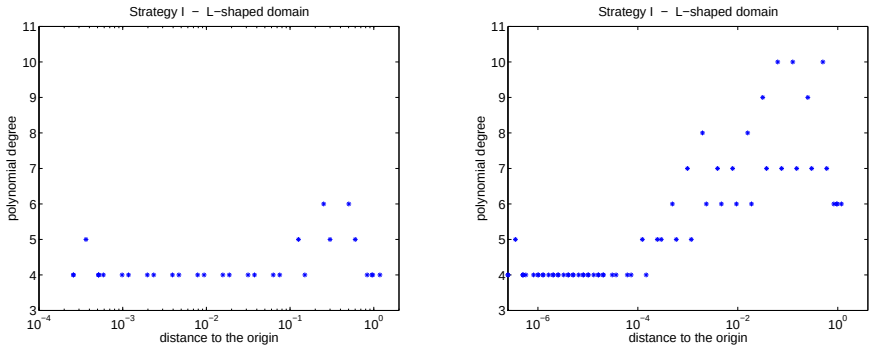

Fig. 17 Strategy II - L-shaped domain - Polynomial degree distribution along the line from (0,0) to (-1/2,1) - Iteration levels 15 and 25

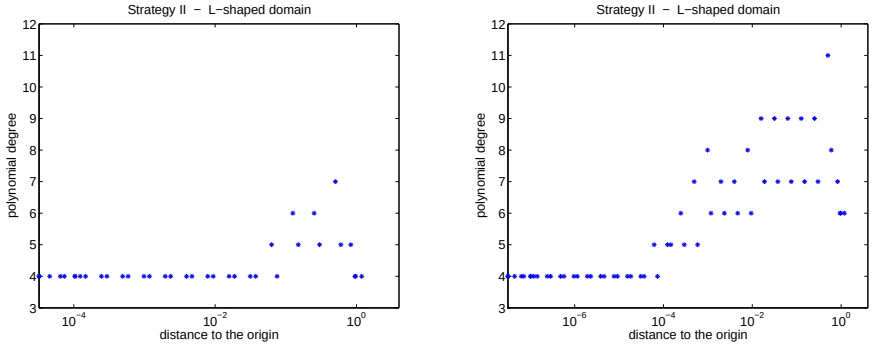

Fig. 18 Strategy III - L-shaped domain - Polynomial degree distribution along the line from (0,0) to (-1/2,1) - Iteration levels 15 and 25

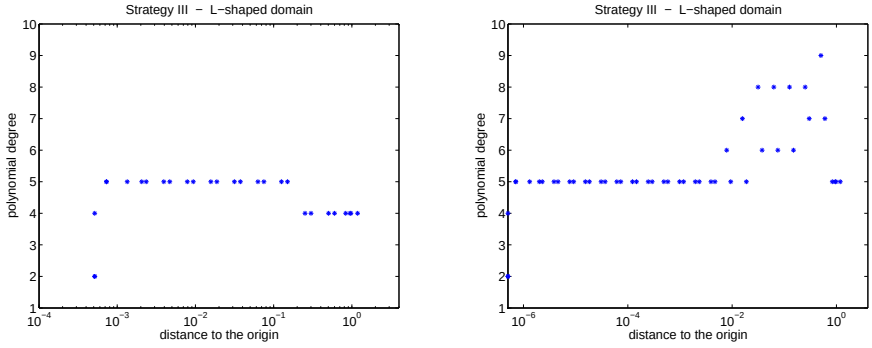

Fig. 19 Comparison - Performance of *hp*-adaptive algorithm

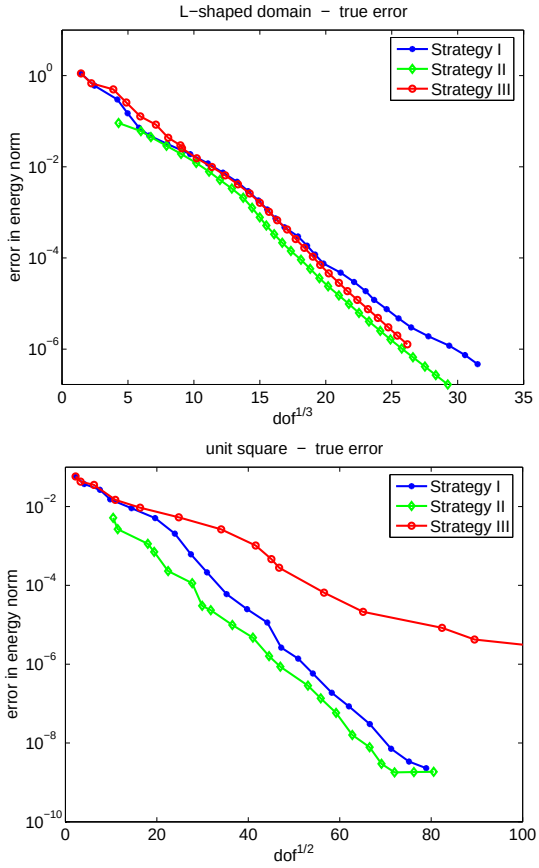

5 Analytic functions on tetrahedra

The *hp*-adaptive strategies of Section 4 can be applied to three-dimensional problems. In this section, we present the theoretical underpinning for the extension to 3D of Strategy II, which relies on estimating the decay of the coefficients when expanding a function in orthogonal polynomials. The main result of the present section is Theorem 1, which is the three-dimensional analog of Proposition 2.

We start with the introduction of some reference elements and transformations:

Definition 4 (reference elements, Duffy transformation) *The reference triangle $\mathcal{T}^2$, the reference tetrahedron $\mathcal{T}^3$ and the i-dimensional reference cube $\mathcal{Q}^i$ are given by:*

$$\begin{aligned}\mathcal{T}^2 &= \{(x,y) \mid -1 < x,y \ \wedge \ x+y < 0\},\\ \mathcal{T}^3 &= \{(x,y,z) \mid -1 < x,y,z \ \wedge \ x+y+z < -1\},\\ \mathcal{Q}^i &= (-1,1)^i.\end{aligned}$$

The transformations D_2, D_3 are given by:

$$D_2 : (\eta_1,\eta_2) \mapsto \left(\frac{1}{2}(1+\eta_1)(1-\eta_2)-1,\eta_2\right),$$
$$D_3 : (\eta_1,\eta_2,\eta_3) \mapsto \left(\frac{1}{4}(1+\eta_1)(1-\eta_2)(1-\eta_3)-1,\frac{1}{2}(1+\eta_2)(1-\eta_3)-1,\eta_3\right),$$

The following lemma links the elements $\mathcal{T}^i$ and $\mathcal{Q}^i$ by means of the Duffy transformations D_i:

Lemma 3 *For $i = 2,3$ let the reference elements $\mathcal{T}^i$, $\mathcal{Q}^i$ and the transformations D_i be given by Definition 4. Then:*

$$\mathcal{T}^i = D_i(\mathcal{Q}^i), \quad i = 2,3. \tag{7}$$

Furthermore, the inverse maps of the $D_i : \mathcal{Q}^i \to \mathcal{T}^i$ are given by

$$D_2^{-1} : (\xi_1,\xi_2) \mapsto \left(2\frac{1+\xi_1}{1-\xi_2}-1,\xi_2\right),$$
$$D_3^{-1} : (\xi_1,\xi_2,\xi_3) \mapsto \left(2\frac{1+\xi_1}{-\xi_2-\xi_3}-1,2\frac{1+\xi_2}{1-\xi_3}-1,\xi_3\right).$$

Proof Direct calculation.

5.1 Orthogonal polynomials on tetrahedra

Similar to the case of the triangle in two dimensions, we introduce the set $(\psi_{pqr})_{p,q,r\in\mathbb{N}_0}$ of polynomials that are orthogonal on the reference tetrahedron.

Definition 5 (orthogonal polynomials on the tetrahedron) *Let D_3 be given by Definition 4 and denote by $P_n^{(\alpha,\beta)}(\eta)$ the n-th Jacobi polynomial with respect to the weight $(1-\eta)^\alpha(1+\eta)^\beta$. Then, for $p,q,r\in\mathbb{N}_0$, we define*

$$\psi_{pqr} = \tilde{\psi}_{pqr}\circ D_3^{-1},$$

where $\tilde{\psi}_{pqr}(\eta) = \tilde{\psi}_{pqr}(\eta_1,\eta_2,\eta_3)$ is given by

$$\tilde{\psi}_{pqr}(\eta) = P_p^{(0,0)}(\eta_1)P_q^{(2p+1,0)}(\eta_2)P_r^{(2p+2q+2,0)}(\eta_3)\left(\frac{1-\eta_2}{2}\right)^p\left(\frac{1-\eta_3}{2}\right)^{p+q}.$$

The following lemma shows that the functions ψ_{pqr} are L^2-orthogonal polynomials on the reference tetrahedron $\mathcal{T}^3$.

Lemma 4 *Let the reference tetrahedron T^3 be given by Definition 4. Then the functions ψ_{pqr} defined in Definition 5 satisfy $\psi_{pqr}\in\mathcal{P}_{p+q+r}(\mathcal{T}^3)$ and they are orthogonal on $\mathcal{T}^3$ with respect to the usual $L^2(\mathcal{T}^3)$ inner product. We have*

$$(\psi_{pqr},\psi_{p'q'r'})_{L^2(\mathcal{T}^3)} = \frac{2}{(2p+1)}\frac{2}{(2p+2q+2)}\frac{2}{(2r+2p+2q+3)}\delta_{p'p}\delta_{q'q}\delta_{r'r}.$$

Proof See [23] together with [25] where a two dimensional version of this Lemma is proved.

5.2 Orthogonal polynomials and analytic functions

The following theorem characterises functions that analytic in a neighbourhood of a tetrahedron:

Theorem 1 *Let the reference element $\mathcal{T}^3$ and the polynomials ψ_{pqr} be given by Definition 4 and Definition 5. Let the function $u\in L^2(\mathcal{T}^3)$ be written as*

$$u = \sum_{p,q,r\in\mathbb{N}_0} u_{pqr}\psi_{pqr}.$$

Then u is analytic on $\overline{\mathcal{T}}^3$ if and only if there exist constants $C,b>0$ such that

$$|u_{pqr}| \le Ce^{-b(p+q+r)} \qquad \forall p,q,r\in\mathbb{N}_0. \tag{8}$$

Before proving this result, we need to introduce some notation. For $\rho > 1$, we let $\mathcal{E}_\rho \subset \mathbb{C}$ be the ellipse with foci ± 1 and sum of semi-axes ρ, i.e.,

$$\mathcal{E}_\rho := \left\{ z \in \mathbb{C} \mid |z+1| + |z-1| < \rho + \rho^{-1} \right\}.$$

A calculation shows that

$$\operatorname{dist}(\partial\mathcal{E}_\rho, 1) = \frac{(\rho-1)^2}{2\rho}.$$

Lemma 5 *For α, $\beta > -1$ denote by $P_q^{(\alpha,\beta)}(\eta)$ the q-th Jacobi polynomial with respect to the weight $(1-\eta)^\alpha(1+\eta)^\beta$. Then, for each $q \in \mathbb{N}_0$, the function*

$$w \mapsto \tilde{Q}_q^{(\alpha,\beta)}(w) = \int_{-1}^{1} (1-t)^\alpha (1+t)^\beta \frac{P_q^{(\alpha,\beta)}(t)}{w-t}\, dt$$

is holomorphic on $\mathbb{C}\backslash[-1,1]$ and for $\rho > 1$ we have

$$\left|\tilde{Q}_q^{(0,0)}(w)\right| \le \frac{2\pi}{1-1/\rho}\rho^{-(q+1)} \quad \forall\, w \in \partial\mathcal{E}_\rho,$$

$$\left|\tilde{Q}_q^{(\alpha,0)}(w)\right| \le \frac{2^{\alpha+2}}{\alpha+1}\frac{q+2}{(1-1/\rho)^2}\rho^{-(q+1)} \quad \forall\, w \in \partial\mathcal{E}_\rho.$$

Proof [25, Lemma 3.2.10, Corollary 3.2.11]

Proof of Theorem 1. First, we assume (8) and show that $\sum_{p,q,r\in\mathbb{N}_0} u_{pqr}\psi_{pqr}$ represents an analytic function. To that end, we chose $\rho > 1$ so small that $\ln\rho \le b/2$ and set

$$u_k := \sum_{p+q+r\le k} u_{pqr}\psi_{pqr}, \qquad k = 0, 1, \ldots, .$$

Lemma 9 ensures the existence of an open complex neighbourhood $\mathcal{T}' \subset \mathbb{C}^3$ of $\overline{\mathcal{T}}^3$ such that

$$\|\psi_{pqr}\|_{L^\infty(\mathcal{T}')} \le e^{(b/2)(p+q+r)}.$$

In combination with (8) we obtain that the sequence $(u_k)_{k=0}^\infty$ converges uniformly on $\mathcal{T}'$. Since all the functions u_k are analytic on $\mathcal{T}'$, the limit function u is analytic on $\mathcal{T}'$ (see, e.g., [20, Cor. 2.2.4]).

We now turn to the second part of the theorem, where we show that analyticity of u on a neighbourhood of the closure of the reference tetrahedron $\mathcal{T}^3$. Since the polynomials ψ_{pqr} are $L^2(\mathcal{T}^3)$-orthogonal, we compute

$$u_{pqr} = \frac{(\psi_{pqr}, u)_{L^2(\mathcal{T}^3)}}{\|\psi_{pqr}\|^2_{L^2(\mathcal{T}^3)}} = \frac{1}{\|\psi_{pqr}\|^2_{L^2(\mathcal{T}^3)}} \int_{\mathcal{T}^3} u\, \psi_{pqr}\, \mathrm{d}\Omega.$$

We need to show the existence of C, $b > 0$ such that

$$\left|(\psi_{pqr}, u)_{L^2(\mathcal{T}^3)}\right| \le Ce^{-b(p+q+r)}. \tag{9}$$

Denoting by U_{pq} the function defined in Lemma 8, the transformation of $\mathcal{T}^3$ to the cube $\mathcal{Q}^3$ via D_3 yields

$$\left|(\psi_{pqr},u)_{L^2(\mathcal{T}^3)}\right| = \left|\int_{-1}^{1} P_r^{(2p+2q+2,0)}(\eta_3)\left(\frac{1-\eta_3}{2}\right)^{(p+q+2)} U_{pq}(\eta_3)\mathrm{d}\eta_3\right|.$$

Lemma 8 asserts that U_{pq} is holomorphic on $\mathcal{E}_\rho$ for some $\rho>1$ and has a zero of multiplicity $p+q$ at $\eta_3=1$. Hence, we may apply Cauchy's integral theorem to the holomorphic function $\eta_3 \mapsto U_{pq}(\eta_3)/(1-\eta_3)^{(p+q)}$ and obtain a first bound for $(\psi_{pqr},u)_{L^2(\mathcal{T}^3)}$:

$$\begin{aligned}
&\left|(\psi_{pqr},u)_{L^2(\mathcal{T}^3)}\right| \qquad (10)\\
&\quad= \left|2^{-p-q-2}\int_{-1}^{1}(1-\eta_3)^{(2p+2q+2)}\,\frac{U_{pq}(\eta_3)}{(1-\eta_3)^{p+q}}P_r^{(2p+2q+2,0)}(\eta_3)\mathrm{d}\eta_3\right|\\
&\quad= \left|\frac{2^{-(p+q+2)}}{2\pi\mathbf{i}}\oint_{\zeta_3\in\partial\mathcal{E}_\rho}\frac{U_{pq}(\zeta_3)}{(1-\zeta_3)^{p+q}}\tilde{Q}_r^{(2p+2q+2,0)}(\zeta_3)\mathrm{d}\zeta_3\right|\\
&\quad\le C2^{-(p+q+2)}\frac{\mathrm{length}(\partial\mathcal{E}_\rho)}{(\mathrm{dist}(\partial\mathcal{E}_\rho,1))^{(p+q)}}\left\|U_{pq}\right\|_{L^\infty(\partial\mathcal{E}_\rho)}\left\|\tilde{Q}_r^{(2p+2q+2,0)}\right\|_{L^\infty(\partial\mathcal{E}_\rho)}\\
&\quad\le C2^{-(p+q+2)}\rho\left(\frac{2\rho}{(\rho-1)^2}\right)^{p+q}e^{-b(p+q)}\frac{2^{(2p+2q+2)}}{(2p+2q+3)}\frac{(r+2)}{(1-1/\rho)^2}\rho^{-(r+1)}\\
&\quad\le C\gamma^{p+q}\delta^{-r}, \qquad (11)
\end{aligned}$$

with $\delta>1$ and C, γ, δ independent of p,q,r. Next, making use of the Cauchy-Schwarz inequality, exploiting orthogonality relations of Jacobi polynomials and Lemma 8 we obtain a second bound for $(\psi_{pqr},u)_{L^2(\mathcal{T}^3)}$

$$\begin{aligned}
\left|(\psi_{pqr},u)_{L^2(\mathcal{T}^3)}\right| &= \left|\int_{-1}^{1}P_r^{(2p+2q+2,0)}(\eta_3)\left(\frac{1-\eta_3}{2}\right)^{(p+q+2)}U_{pq}(\eta_3)\mathrm{d}\eta_3\right|\\
&\le \left(\int_{-1}^{1}\left(\frac{1-\eta_3}{2}\right)^{(2p+2q+2)}\left(P_r^{(2p+2q+2,0)}(\eta_3)\right)^2\mathrm{d}\eta_3\right)^{\frac12}\times\\
&\quad\left(\int_{-1}^{1}\left(\frac{1-\eta_3}{2}\right)^{2}|U_{pq}(\eta_3)|^2\mathrm{d}\eta_3\right)^{\frac12}\\
&\le C\left(\frac{2}{2p+2q+2r+3}\right)^{\frac12}e^{-b(p+q)}\le Ce^{-b(p+q)}. \qquad (12)
\end{aligned}$$

We combine inequality (11) and (12) to achieve

$$|u_{pqr}|\le C\min\{e^{-b(p+q)},\gamma^{p+q}\delta^{-r}\}. \qquad (13)$$

If $\gamma<1$, then (13) implies immediately (9). We may therefore assume $\gamma\ge1$. Since $\delta>1$, we may choose $\lambda\in(0,1]$ such that $\gamma^\lambda/\delta =: q<1$. Then, we distinguish two cases:

1. For $(p+q) \leq \lambda r$ we have

$$|u_{pqr}| \leq C\gamma^{p+q}\delta^{-r} \leq C(\gamma^{\lambda}/\delta)^r = Cq^r = Cq^{r/2+r/2} \leq Cq^{\frac{1}{2}(r+p+q)},$$

   which is the desired bound (9).
2. For $(p+q) > \lambda r$ we have

$$(p+q) \geq \frac{\lambda}{2}(p+q+r),$$

   and the desired result follows from

$$|u_{pqr}| \leq Ce^{-b(p+q)} \leq Ce^{-b\frac{\lambda}{2}(p+q+r)} \leq Ce^{-b'(p+q+r)}.$$

5.3 Auxiliary Results

Lemma 6 *Let D_3 be given by Definition 4 and let u be analytic on $\overline{\mathcal{T}}^3$. Then there exist $C > 0$, $\delta > 0$, $\rho > 1$ depending only on u such that:*

(i) The function $u \circ D_3$ is holomorphic on $\overline{\mathcal{Q}}^3$ and can be extended to a function $\tilde{u}$ holomorphic on $\mathcal{E}_\rho \times \mathcal{E}_\rho \times \mathcal{E}_\rho$ with

$$\|\tilde{u}\|_{L^\infty(\mathcal{E}_\rho^3)} \leq C.$$

(ii) For all $\eta_2, \eta_3 \in (-1,1)$ the function $\eta_1 \mapsto \tilde{u}(\eta_1, \eta_2, \eta_3)$ is holomorphic on $\mathcal{E}_{1+\delta/((1-\eta_2)(1-\eta_3))}$ and we have

$$\sup_{(\eta_2,\eta_3)\in\mathcal{Q}^2} \|\tilde{u}(\cdot, \eta_2, \eta_3)\|_{L^\infty(\mathcal{E}_{1+\delta/((1-\eta_2)(1-\eta_3))})} \leq C.$$

(iii) For all $\eta_1, \eta_3 \in (-1,1)$ the function $\eta_2 \mapsto \tilde{u}(\eta_1, \eta_2, \eta_3)$ is holomorphic on $\mathcal{E}_{1+\delta/(1-\eta_3)}$ and we have

$$\sup_{(\eta_1,\eta_3)\in\mathcal{Q}^2} \|\tilde{u}(\eta_1, \cdot, \eta_3)\|_{L^\infty(\mathcal{E}_{1+\delta/(1-\eta_3)})} \leq C.$$

Proof Since u is analytic on $\overline{\mathcal{T}}^3$, there exists a complex open neighbourhood $\mathcal{T}' \subset \mathbb{C}^3$ of $\overline{\mathcal{T}}^3$ such that u is holomorphic and bounded on $\mathcal{T}'$. Thus, because of the continuity of D_3, there exists $\rho > 1$ such that $D_3(\mathcal{E}_\rho^3) \subset \mathcal{T}'$ and the first claim is proved. In order to prove the second claim, we have to show that for arbitrary $\epsilon > 0$ there exists $\delta(\epsilon) > 0$ such that

$$(\eta_1, \eta_2, \eta_3) \in G_\delta := \left\{(\eta_1, \eta_2, \eta_3) \mid \eta_1 \in \mathcal{E}_{\rho_1}, (\eta_2, \eta_3) \in \mathcal{Q}^2\right\}$$

with

$$\rho_1 = 1 + \frac{\delta}{(1-\eta_2)(1-\eta_3)} \tag{14}$$

implies

$$\inf_{\mathbf{x}\in\overline{\mathcal{T}}^3} |D_3(\eta_1, \eta_2, \eta_3) - \mathbf{x}| \leq \epsilon. \tag{15}$$

To that end, we set $\eta_1 = a + b\mathbf{i}$, $\delta < \frac{8}{\sqrt{5}}\epsilon$ and distinguish three cases:

1. For $a \le -1$ we have $A_1 := D_3(-1,\eta_2,\eta_3) \in \overline{\mathcal{T}}^3$ with:

$$\begin{aligned}
&|D_3(\eta_1,\eta_2,\eta_3) - A_1| \\
&\quad = \frac{1}{4}(1-\eta_2)(1-\eta_3)|\eta_1+1| \le \frac{\sqrt{5}}{4}(1-\eta_2)(1-\eta_3)\left|\frac{1}{2}(\rho_1+\rho_1^{-1})-1\right| \\
&\quad = \frac{1}{4}(1-\eta_2)(1-\eta_3)\frac{\sqrt{5}}{2}\frac{\delta}{(1-\eta_2)(1-\eta_3)}\cdot\frac{\delta}{(1-\eta_2)(1-\eta_3)+\delta} < \epsilon.
\end{aligned}$$

2. For $|a| < 1$ we have $A_2 := D_3(a,\eta_2,\eta_3) \in \overline{\mathcal{T}}^3$ with:

$$\begin{aligned}
&|D_3(\eta_1,\eta_2,\eta_3) - A_2| \\
&\quad = \frac{1}{4}(1-\eta_2)(1-\eta_3)|b| \le \frac{1}{8}(1-\eta_2)(1-\eta_3)|\rho_1-\rho_1^{-1}| \\
&\quad = \frac{1}{8}(1-\eta_2)(1-\eta_3)\left|\frac{\delta}{(1-\eta_2)(1-\eta_3)}\cdot\frac{2(1-\eta_2)(1-\eta_3)+\delta}{(1-\eta_2)(1-\eta_3)+\delta}\right| < \epsilon.
\end{aligned}$$

3. For $a \ge 1$ we have $A_3 := D_3(1,\eta_2,\eta_3) \in \overline{\mathcal{T}}^3$ and obtain analogously to the case $a \le -1$:

$$|D_3(\eta_1,\eta_2,\eta_3) - A_3| \le \frac{\sqrt{5}}{8}\delta < \epsilon.$$

To prove the third claim we proceed similarly.

Lemma 7 *Let the transformation D_3 be given by Definition 4 and let the function u be analytic on $\overline{\mathcal{T}}^3$. For $p \in \mathbb{N}_0$ let the function $(\eta_2,\eta_3) \mapsto U_p(\eta_2,\eta_3)$ be defined by:*

$$U_p(\eta_2,\eta_3) := \int_{-1}^{1} P_p^{(0,0)}(\eta_1)[u \circ D_3](\eta_1,\eta_2,\eta_3)\,d\eta_1.$$

Then there exist $\rho > 1$, $\delta > 0$, $C > 0$ depending only on u such that:

(i) The function U_p is holomorphic and bounded on $\mathcal{E}_\rho \times \mathcal{E}_\rho$ with

$$\|U_p\|_{L^\infty(\mathcal{E}_\rho\times\mathcal{E}_\rho)} \le C\rho^{-p}.$$

(ii) For each $\eta_3 \in (-1,1)$ the function $\eta_2 \mapsto U_p(\eta_2,\eta_3)$ is holomorphic on $\mathcal{E}_{1+\delta/(1-\eta_3)}$ with

$$\sup_{\eta_3\in(-1,1)} \|U_p(\cdot,\eta_3)\|_{L^\infty(\mathcal{E}_{1+\delta/(1-\eta_3)})} \le C.$$

(iii) The function U_p has zeros of multiplicity p at $\eta_2 = 1$ and $\eta_3 = 1$.

Proof The second claim follows from Lemma 6, (iii) and U_p holomorphic on $\mathcal{E}_\rho \times \mathcal{E}_\rho$ follows from Lemma 6, (i). To prove $\|U_p\|_{L^\infty(\mathcal{E}_\rho \times \mathcal{E}_\rho)} \leq C\rho^{-p}$, we exploit Cauchy's integral representation formula and obtain with Lemma 5:

$$\begin{aligned}
|U_p(\zeta_2,\zeta_3)| &= \left| \frac{1}{2\pi\mathbf{i}} \int_{-1}^{1} \oint_{\zeta_1 \in \partial\mathcal{E}_\rho} \frac{\tilde{u}(\zeta_1,\zeta_2,\zeta_3)}{\zeta_1-\eta_1} P_p^{(0,0)}(\eta_1) \mathrm{d}\zeta_1 \mathrm{d}\eta_1 \right| \\
&= \left| \frac{1}{2\pi\mathbf{i}} \oint_{\zeta_1 \in \partial\mathcal{E}_\rho} \tilde{u}(\zeta_1,\zeta_2,\zeta_3) \tilde{Q}_p^{(0,0)}(\zeta_1) \mathrm{d}\zeta_1 \right| \\
&\leq \frac{\mathrm{length}(\mathcal{E}_\rho)}{2\pi} \|\tilde{u}\|_{L^\infty(\mathcal{E}_\rho^3)} \|\tilde{Q}_p^{(0,0)}\|_{L^\infty(\partial\mathcal{E}_\rho)} \leq C\rho^{-p},
\end{aligned}$$

By Lemma 7, (i) U_p is holomorphic on $\mathcal{E}_\rho \times \mathcal{E}_\rho$. In order to show that it has a zero of multiplicity p at $\eta_2 = 1$ and $\eta_3 = 1$, it suffices to prove the existence of $C > 0$ independent of η_2, η_3 such that

$$|U_p(\eta_2,\eta_3)| \leq C(1-\eta_2)^p(1-\eta_3)^p \qquad \forall \eta_2,\eta_3 \in (-1,1).$$

Lemma 6, (ii) together with Cauchy's integral representation formula yields

$$|U_p(\eta_2,\eta_3)| = \left| \frac{1}{2\pi\mathbf{i}} \int_{-1}^{1} \oint_{\zeta_1 \in \partial\mathcal{E}_{\rho_1}} \frac{\tilde{u}(\zeta_1,\eta_2,\eta_3)}{\zeta_1-\eta_1} P_p^{(0,0)}(\eta_1) \mathrm{d}\zeta_1 \mathrm{d}\eta_1 \right|$$

with ρ_1 given by (14). Appealing again to Lemma 5, we get

$$\begin{aligned}
|U_p(\eta_2,\eta_3)| &\leq \frac{\mathrm{length}(\partial\mathcal{E}_{\rho_1})}{2\pi} \|\tilde{u}\|_{L^\infty(G_\delta)} \|\tilde{Q}_p^{(0,0)}\|_{L^\infty(\partial\mathcal{E}_{\rho_1})} \\
&\leq C \left(\frac{(1-\eta_2)(1-\eta_3)}{\delta + (1-\eta_2)(1-\eta_3)} \right)^p,
\end{aligned}$$

where C depends solely on u. Since $\delta > 0$ and $\eta_2, \eta_3 \in (-1,1)$, we arrive at

$$|U_p(\eta_2,\eta_3)| \leq C\delta^{-p}(1-\eta_2)^p(1-\eta_3)^p,$$

which is the desired bound.

Lemma 8 *Let the transformation D_3 be given by Definition 4 and let the function u be analytic on $\overline{\mathcal{T}}^3$. For $p,q \in \mathbb{N}_0$ let the function $\eta_3 \mapsto U_{pq}(\eta_3)$ be defined by:*

$$U_{pq}(\eta_3) = \int_{-1}^{1} U_p(\eta_2,\eta_3) P_q^{(2p+1,0)}(\eta_2) \left(\frac{1-\eta_2}{2} \right)^{p+1} d\eta_2,$$

where U_p denotes the function of Lemma 7. Then there exist $\rho > 1$, $b > 0$, $C > 0$ depending only on u such that:

(i) The function U_{pq} is holomorphic on $\mathcal{E}_\rho$ and has a zero of multiplicity $(p+q)$ at $\eta_3 = 1$.
(ii) For all $\zeta_3 \in \mathcal{E}_\rho$

$$|U_{pq}(\zeta_3)| \le Ce^{-b(p+q)}.$$

Proof The holomorphy of U_{pq} follow from Lemma 7, (i). To show that U_{pq} has a zero of multiplicity $(p+q)$ at $\eta_3 = 1$, it suffices to show the existence of C independent of η_3 such that

$$|U_{pq}(\eta_3)| \le C(1-\eta_3)^{p+q} \qquad \forall\, \eta_3 \in (-1,1).$$

From Lemma 7 we know that for each $\eta_3 \in (-1,1)$ the function $U_p(\cdot,\eta_3)$ is holomorphic on $\mathcal{E}_{\rho_2} = \mathcal{E}_{1+\delta/(1-\eta_3)}$ and has a zero of multiplicity p at $\eta_2 = 1$. Hence, we may apply Cauchy's integral theorem to the holomorphic function $\eta_2 \mapsto U_p(\eta_2,\eta_3)/(1-\eta_2)^p$ to arrive at

$$\begin{aligned} U_{pq}(\eta_3) &= \frac{1}{2\pi\mathbf{i}}\left(\frac{1}{2}\right)^{p+1} \oint_{\zeta_2\in\partial\mathcal{E}_{\rho_2}} \frac{U_p(\zeta_2,\eta_3)}{(1-\zeta_2)^p} \int_{-1}^{1} \frac{P_q^{(2p+1,0)}(\eta_2)}{\zeta_2-\eta_2}(1-\eta_2)^{2p+1}\mathrm{d}\eta_2\mathrm{d}\zeta_2 \\ &= C \oint_{\zeta_2\in\partial\mathcal{E}_{\rho_2}} \frac{U_p(\zeta_2,\eta_3)}{(1-\zeta_2)^p}\tilde{Q}_q^{(2p+1,0)}(\zeta_2)\mathrm{d}\zeta_2. \end{aligned} \tag{16}$$

Thus, we obtain

$$\begin{aligned} |U_{pq}(\eta_3)| &\le C\frac{\mathrm{length}(\partial\mathcal{E}_{\rho_2})}{(\mathrm{dist}(\partial\mathcal{E}_{\rho_2},1))^p}\|\tilde{Q}_q^{(2p+1,0)}\|_{L^\infty(\partial\mathcal{E}_{\rho_2})}\,\|U_p(\cdot,\eta_3)\|_{L^\infty(\mathcal{E}_{\rho_2})} \\ &\le C\rho_2\left(\frac{(\rho_2-1)^2}{2\rho_2}\right)^{-p}\left(\frac{2^{2p+3}}{2p+2}\frac{q+2}{(1-1/\rho_2)^2}\rho_2^{-(q+1)}\right) \\ &\le C\frac{\rho_2^{p-q+2}}{(\rho_2-1)^{2p+2}} \le C\frac{(1-\eta_3+\delta)^{p-q+2}}{\delta^{2p+2}}(1-\eta_3)^{p+q} \end{aligned}$$

where C is independent of η_3. Since $\delta > 0$ and $\eta_3 \in (-1,1)$, we arrive at

$$|U_{pq}(\eta_3)| \le C(1-\eta_3)^{p+q},$$

which is the desired bound. We proceed similarly for the second claim. We use the bound (16) but take as the contour of integration $\partial\mathcal{E}_\rho$, i.e.,

$$\begin{aligned} |U_{pq}(\zeta_3)| &= C\left|\oint_{\zeta_2\in\partial\mathcal{E}_\rho} \frac{U_p(\zeta_2,\zeta_3)}{(1-\zeta_2)^p}\tilde{Q}_q^{(2p+1,0)}(\zeta_2)\mathrm{d}\zeta_2\right| \\ &\le C\frac{\mathrm{length}(\partial\mathcal{E}_\rho)}{(\mathrm{dist}(\partial\mathcal{E}_\rho,1))^p}\|\tilde{Q}_q^{(2p+1,0)}\|_{L^\infty(\partial\mathcal{E}_\rho)}\,\|U_p(\zeta_2,\zeta_3)\|_{L^\infty(\mathcal{E}_\rho^2)} \\ &\le C\rho\left(\frac{2\rho}{(\rho-1)^2}\right)^p \frac{2^{2p+3}}{2p+2}\frac{q+2}{(1-1/\rho)^2}\rho^{-(q+1)} \le C\rho^{-q}\gamma^p, \end{aligned}$$

with C, γ independent of p, q, and ζ_3. A second bound for $|U_{pq}(\zeta_3)|$ follows from the Cauchy-Schwarz inequality together with Lemma 7, (i) and basic properties of Jacobi polynomials:

$$\begin{aligned}
|U_{pq}(\zeta_3)| &= \int_{-1}^{1} U_p(\eta_2,\zeta_3) P_q^{(2p+1,0)}(\eta_2) \left(\frac{1-\eta_2}{2}\right)^{p+1} \mathrm{d}\eta_2 \\
&\leq \left\{ \int_{-1}^{1} |U_p(\eta_2,\zeta_3)|^2 \left(\frac{1-\eta_2}{2}\right) \mathrm{d}\eta_2 \right\}^{\frac{1}{2}} \times \\
&\quad \left\{ \int_{-1}^{1} \left(P_q^{(2p+1,0)}(\eta_2)\right)^2 \left(\frac{1-\eta_2}{2}\right)^{2p+1} \mathrm{d}\eta_2 \right\}^{\frac{1}{2}} \\
&\leq C\rho^{-p} \frac{2}{2p+2q+2} \leq C\rho^{-p}.
\end{aligned}$$

Combining the last two bounds as in Theorem 1 gives the desired result

$$|U_{pq}(\zeta_3)| \leq Ce^{-b(p+q)} \qquad \forall \zeta_3 \in \mathcal{E}_\rho.$$

Lemma 9 *Let ψ_{pqr} be given by Definition 5. Then for arbitrary $\rho > 1$ there exists C and an open complex neighbourhood $\mathcal{T}' \subset \mathbb{C}^3$ with $\overline{\mathcal{T}}^3 \subset \mathcal{T}'$ such that*

$$\|\psi_{pqr}\|_{L^\infty(\mathcal{T}')} \leq C(p+q+r)^3 \rho^{p+q+r} \quad \forall p,q,r \in \mathbb{N}_0.$$

Proof For univariate polynomials we have (see [13, Chap 4, Thm. 2.2])

$$\|u\|_{L^\infty(\mathcal{E}_\rho)} \leq \rho^p \|u\|_{L^\infty(-1,1)} \qquad \forall \rho > 1 \quad \forall u \in \mathcal{P}_p.$$

Thus, by tensor product arguments, we obtain

$$\|u\|_{L^\infty(\mathcal{E}^3_{\rho^{1/3}})} \leq \rho^p \|u\|_{L^\infty(\mathcal{Q}^3)} \qquad \forall \rho > 1 \quad \forall u \in Q_p(\mathcal{Q}^3),$$

which implies that for arbitrary $\rho > 1$ there exists an open complex neighbourhood $\mathcal{Q}' \supset \overline{\mathcal{Q}}^3$ such that

$$\|u\|_{L^\infty(\mathcal{Q}')} \leq \rho^p \|u\|_{L^\infty(\overline{\mathcal{Q}}^3)} \qquad \forall u \in Q_p(\mathcal{Q}^3). \tag{17}$$

An affine change of variables shows that (17) holds for an arbitrary closed parallelepiped P. That is, for all $\rho > 1$ there exists an open complex neighbourhood P' of P such that

$$\|u\|_{L^\infty(P')} \leq \rho^p \|u\|_{L^\infty(\overline{P})} \qquad \forall u \in Q_p(\mathcal{Q}^3). \tag{18}$$

Since it is possible to find, for example, ten not necessarily disjoint parallelepipeds $P^1,\ldots,P^{10}$ such that

$$\overline{\mathcal{T}}^3 = \bigcup_{i=1}^{10} \overline{P}^i,$$

we obtain for each $\rho > 1$ a complex neighbourhood $\mathcal{T}' := \cup_{i=1}^{10} P'^i$ of $\overline{\mathcal{T}}^3$ with P'^i given by (18) and

$$\|u\|_{L^\infty(\mathcal{T}')} = \max_{i=1}^{10} \|u\|_{L^\infty(P'^i)} \le \rho^p \max_{i=1}^{10} \|u\|_{L^\infty(\overline{P}^i)} \le \rho^p \|u\|_{L^\infty(\overline{\mathcal{T}}^3)} \tag{19}$$

for all $u \in \mathcal{P}_p(\mathcal{T}^3)$. In order to replace the L^∞ bound on the right-hand side by an L^2-bound, we need the following polynomial inverse estimate:

$$\|u\|_{L^\infty(\overline{\mathcal{T}}^3)} \le Cp^3 \|u\|_{L^2(\overline{\mathcal{T}}^3)} \qquad \forall\, u \in \mathcal{P}_p(\mathcal{T}^3); \tag{20}$$

this estimate can be obtained using the same arguments as in the two-dimensional situation proved in [30, Thm. 4.76]. Inserting (20) into (19) gives for the polynomial ψ_{pqr}

$$\|\psi_{pqr}\|_{L^\infty(\mathcal{T}')} \le C(p+q+r)^3 \rho^{p+q+r} \|\psi_{pqr}\|_{L^2(\mathcal{T}^3)}.$$

The claim of the lemma now follows from Lemma 4, which gives us the bound $\|\psi_{pqr}\|_{L^2(\mathcal{T}^3)} \le 2/\sqrt{3}$ for all $p, q, r \in \mathbb{N}_0$.

References

1. M. Ainsworth and B. Senior. Aspects of an adaptive *hp*-finite element method: adaptive strategy, conforming approximation and efficient solvers. *Comput. Meth. Appl. Mech. Engrg.*, 150:65–87, 1997.
2. M. Ainsworth and B. Senior. An adaptive refinement strategy for *hp*-finite-element computations. *Appl. Numer. Math.*, 26:165—178, 1998.
3. M. Ainsworth and B. Senior. *hp*-finite element procedures on non-uniform geometric meshes. In M. Bern, J. Flaherty, and M. Luskin, editors, *Grid generation and adaptive algorithms*, pages 1–27. Springer Verlag, 1999. IMA Vol. Math. Appl. 113.
4. T. Apel. *Anisotropic Finite Elements: Local Estimates and Applications.* Advances in Numerical Mathematics. Teubner, 1999.
5. T. Apel, S. Grosmann, P. Jimack, and A. Meyer. A new methodology for anisotropic mesh refinement based upon error gradients. *Appl. Numer. Math.*, 50:329–341, 2004.
6. I. Babuška and B.Q. Guo. The $h-p$ version of the finite element method. Part 1: The basic approximation results. *Computational Mechanics*, 1:21–41, 1986.
7. I. Babuška and M. Suri. The optimal convergence rate of the *p*-version of the finite element method. *SIAM J. Numer. Anal.*, 24:750–776, 1987.
8. C. Bernardi, R.G. Owens, and J. Valenciano. An error indicator for mortar element solutions to the Stokes problem. *IMA J. Numer. Anal.*, 21:857–886, 2001.
9. E. Bertóti and B. Szabó. adaptive selection of polynomial degrees on a finite element mesh. *Internat. J. Numer. Meths. Engrg.*, 42:561–578, 1998.
10. E. Creusé, G. Kunert, and S. Nicaise. A posteriori error estimation for the Stokes problem: anisotropic and isotropic discretizations. *Math. Meths. Appl. Sci.*, 14:1297–1341, 2004.

11. L. Demkowicz, W. Rachowicz, and Ph. Devloo. A fully automatic *hp*-adaptivity. *J. Sci. Comput.*, 17:117–142, 2002.
12. L. Demkowicz and P. Solin. Goal oriented hp-adaptivity for elliptic problems. *Comput. Meth. Appl. Mech. Engrg.*, 193:449–468, 2004.
13. R.A. DeVore and G.G. Lorentz. *Constructive Approximation*. Springer Verlag, 1993.
14. T. Eibner. *Algorithmik der randkonzentrierten FEM*. PhD thesis, Technische Universität Chemnitz, (in prep.).
15. T. Eibner and J.M. Melenk. Fast algorithms for setting up the stiffness matrix in *hp*-fem: a comparison. (in prep.).
16. L. Formaggia, S. Micheletti, and S. Perotto. Anisotropic mesh adaption in computational fluid dynamics: application to the advection-diffusion-reaction and the Stokes problems. *Appl. Numer. Math.*, 51:511–533, 2004.
17. H. Goering, H.G. Roos, and L. Tobiska. *Finite-Element-Methode*. Akademie-Verlag, 1993.
18. N. Heuer, M.E. Mellado, and E.P. Stephan. *hp*-adaptive two-level methods for boundary integral equations on curves. *Computing*, 67(4):305–334, 2001.
19. V. Heuveline and R. Rannacher. Duality-based adaptivity in the *hp*-finite element method. *J. Numer. Math.*, 11(2), 2003.
20. L. Hörmander. *An Introduction to Complex Analysis in Several Variables*. North Holland, 1990.
21. P. Houston, B. Senior, and E. Süli. Sobolev regularity estimation for hp-adaptive finite element methods. In F. Brezzi, A. Buffa, S. Corsaro, and A. Murli, editors, *Numerical Mathematics and Advanced Applications, ENUMATH 2001*, pages 631–656. Springer-Verlag, 2003.
22. P. Houston and E. Süli. A note on the design of *hp*-adaptive finite element methods for elliptic partial differential equations. *Comput. Meth. Appl. Mech. Engrg.*, 194:229–243, 2005.
23. G.E. Karniadakis and S.J. Sherwin. *Spectral/hp Element Methods for CFD*. Oxford University Press, 1999.
24. Catherine Mavriplis. Adaptive mesh strategies for the spectral element method. *Comput. Methods Appl. Mech. Engrg.*, 116(1-4):77–86, 1994. ICOSAHOM'92 (Montpellier, 1992).
25. J.M. Melenk. *hp finite element methods for singular perturbations*, volume 1796 of *Lecture Notes in Mathematics*. Springer Verlag, 2002.
26. J.M. Melenk, K. Gerdes, and C. Schwab. Fully discrete *hp*-FEM: fast quadrature. *Comput. Meth. Appl. Mech. Engrg.*, 190:4339–4364, 2001.
27. J.M. Melenk and B. Wohlmuth. On residual-based a posteriori error estimation in *hp*-FEM. *Advances in Comp. Math.*, 15:311–331, 2001.
28. J.T. Oden, W. Wu, and M. Ainsworth. Three-step *hp* adaptive strategy for the incompressible Navier-Stokes equations. In I. Babuška, J. Flaherty, W. Henshaw, J. Hopcroft, J. Oliger, and T. Tezduyar, editors, *Modeling, Mesh Generation, and Adaptive Numerical Methods for Partial Differential Equations*, pages 347–366. Springer-Verlag, 1995.
29. T.J. Oden, A. Patra, and Y.S. Feng. An *hp* adaptive strategy. In A.K. Noor, editor, *Adaptive, Multilevel and Hierarchical Computational Strategies*, pages 23–46. ASME Publications, 1993.
30. C. Schwab. *p- and hp-Finite Element Methods*. Oxford University Press, 1998.